한국가시화정보학회지, 제7권, 제1호, (2009) 21~28
<일반논문> (투고일: 2009.05.25/수정일: 2009.07.30/심사완료일: 2009.08.04)

Review of Experimental Studies on Swirling Flow in the Circular Tube using PIV Technique

Tae-Hyun Chang†, Do-Baek Nah* and Sang Woo Kim*

Abstract. The study of swirling flow is of technical and scientific interest because it has an internal recirculation field, and its tangential velocity is related to the curvature of streamline. The fluid flow for tubes and elbow of heat exchangers has been studied largely through experiments and numerical methods, but studies about swirling flow have been insufficient. Using the particle image velocimetry(PIV) method, this study found the time averaged velocity distribution with swirl and without swirl along longitude sections and the results appear to be physically reasonable. In addition, streamwise mean velocity distribution was compares with that of other. Furthermore, other experimental investigation was performed to study the characteristics of turbulent water flow in a horizontal circular tube by using liquid crystal. 2D PIV technique is employed for velocity measurement and liquid crystal is used for heat transfer experiments in water. Temperature visualization was made quantitatively by calibrating the colour of the liquid crystal versus temperature using various approaches.

Key Words: Swirling flow, PIV, liquid crystal

NOMENCLATURE

D: Diameter of the concave tube(mm)
d: Diameter of the convex tube(mm)
L: Axial distance of the swirl chamber(mm)
R: Radius of the concave tube(mm)
r: Radius of the convex tube(mm)
U: Time averaged axial velocity(m/s)
u, v ,w: Fluctuating velocity(m/s)
V: Time averaged radial velocity(m/s)
X: Axial coordinate of the test tube(mm)
y: Radial position from the wall(mm)
S: Swirl intensity($S = 1/R\left[\int_0^r uwr^2 / \int_0^r u^2 r dr\right]$)
θ: Swirl angle($\theta = tan^{-1}\frac{vw}{uv}$)
Subscripts
o: outlet
i: inside

†Senior Research Fellow, RESEAT, KISTI
E-mail : changtae@kyungnam.ac.kr
*Principal researcher of KISTI

1. Introduction

During the past three decade or so, the characteristics of turbulent swirling flow have been studied extensively because of its great technological and scientific importance. It is well known that swirling flow improves heat transfer in duct flow. The reason for this is due to the effect of streamline curvature associate with the tangential velocity component. Many experimental investigations have been carried out in turbulent swirling flow with and without heat transfer. A large proportion of them deal specifically with the type of swirl conditions that exist in combustion situations, and these are summarized in the excellent review paper of Lilley[1]. One of the earliest important studies by Nuttall[2] in 1953. He was one of the first to observe the flow characteristics of swirling flow in circular tubes by using flow visualization techniques(dye injection method). In this respect, the early studies such as those of Binnie et al[3] and Chigier et al[4], used pitot tubes. Others such as Nuttall[1], Binnie et al[3] and Sparrow et al[5] used flow visualization techniques similar to Nuttall's experiments to confirm the existence of flow reversal regimes.

Recently, Chang et al[6] used PIV(particle image velocimetry) technique with swirl flow and without swirl in circular tubes.

Chigier et al[7], Scott et al[8], Milar[9], Clayton et al[10] and Reddy et al[11] studied about the swirl flow through a cylindrical annuli by measuring velocity profiles and pressure losses and applyed the numerical analysis method. Recently, Chang et. al[6] calculated the velocity profiles and Reynolds stress in the horizontal cylindrical annuli by the particle image velocimetry method. but there is seldom an investigation done in this area. Thus, this study was performed to investigate the characteristics of swirl flow through visualization experiments of air and water flow, which is carried out by using smoke and dye in the horizontal annuli of radius ratio Ro/Ri = 3.0, and to measure the static pressure, the local flow temperature and the tube wall temperature of swirl and without swirl flow of Re = 30,000~80,000(or Re=60,000~100,000 for swirl angle measurement with air) under a uniform heat flux, to find out the Nusselt number and to contribute to the compact and economical design of heat exchangers.

2. Experimental rig for a single straight tube

Fig. 1 shows the layout of experimental apparatus used in this study for a single straight tube. The experimental rig was manufactured from an acryl tube. Water was drawn through a swirl generating chamber, the test tube working section, flow metering and main plenum chamber by a centrifugal pump. Adjustment of the rpm controller on the water pump discharge side provides a coarse variation of water flow rate, with finer control being achieved with a valve located in the side of the plenum chamber. The isothermal test section was of 50.8 mm inside diameter with a wall thickness of 6.36 mm and length of 3 m, and was manufactured from acryl tube. Fig. 2 is showing the swirl generator. The swirl generator consisted of two perspex cylinder of following dimensions an outer chamber of outsider diameter 241 mm, length 106.9 mm and thickness 6.35 mm: the swirl generator itself of outside diameter 165.6 mm, length 250 mm and wall thickness 6.35 mm.

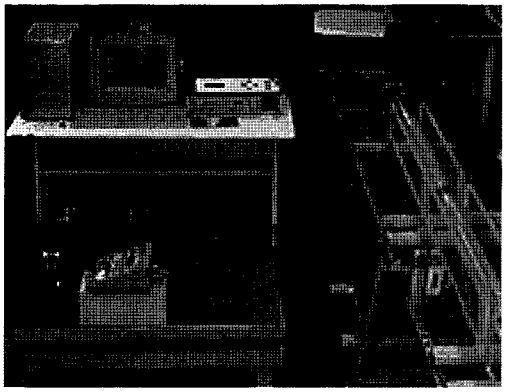

Fig. 1. Experimental Apparatus for Swirling flow

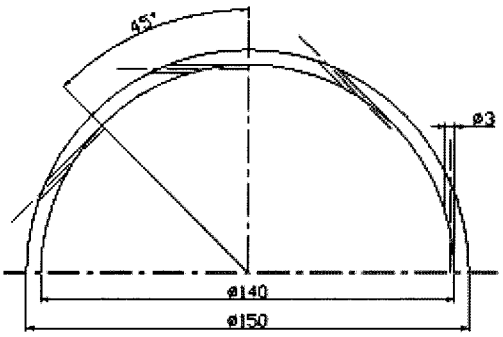

Fig. 2. The cross section view of swirl generator

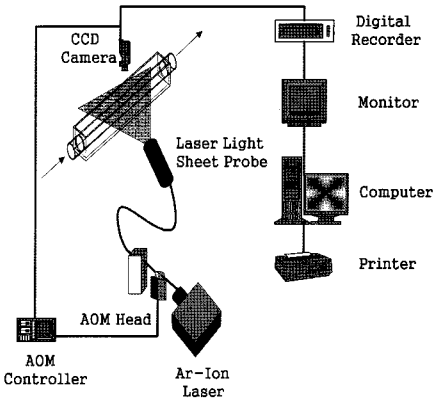

Fig. 3. Schematic arrangement of PIV system

2.1 Experiment method

To determine some characteristics of the swirl flow induce by the swirl chamber used in this investigation, the flow visualization experiments are carried out first using smoke and dye liquid. The velocities are measured using 2-D PIV tech-

nique and swirl motion of fluid is produced by tangential inlet condition. The source of light which is used in this research is an air-cooling, 500 mW and 2W, Air-ion laser. Laser light sheet probe is employed to move the source easily by using optical cable and Acoustic Optical Modulator is used to got be pulsed laser light source. The observation is made by a CCD camera having a DT3155 board, which is operated in 640×480 pixel as like Fig. 3.

3. Results and Discussion

3.1 Velocity vector profiles for circular tube

Fig. 4 shows the data of velocity vectors, X/D= 10, 16, 24, 36, 44 and 50 by PIV method. Even though the flow shows intensive swirling at the inlet of the test tube, its swirl flow intensity is gradually reduced according to the flow through tube, and at the end of tube swirl movements is diminished and changed to a uniform flow.

Some of first measurement indicated that over the first 4 diameter, two regions of flow reversal

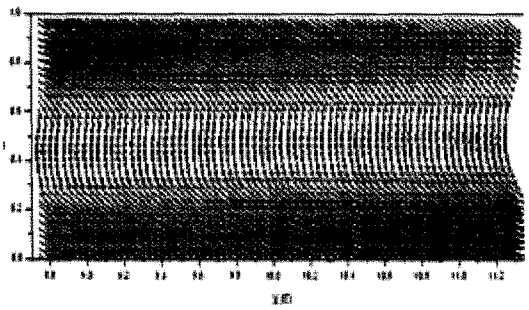

Fig. 4. Mean velocity vectors along the test Tube with swirl at x/D=10 for Re=10,000

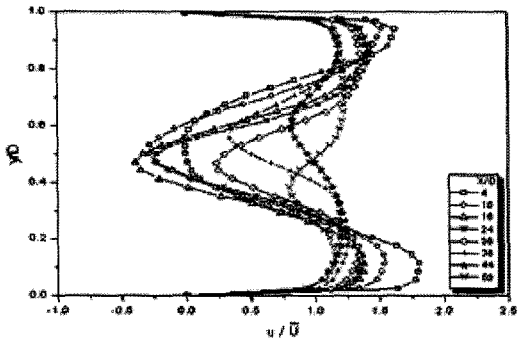

Fig. 5. Axial velocity profiles with swirl for Re=10,000 along the test tube

were set up(the so called 2-cell structure). When the Reynolds number was higher, the intensity of swirling at the tube inlet was increased. By this effect, it can be considered that there is negative velocity at tube inlet.

The sequence of velocity distributions show on Fig. 5 clearly demonstrates that flow reversal becomes diminished and finally disappears with axial distance from the inlet, as the swirl is reduce(i.e. L/D increases).

3.2 Velocity profiles in an annuli

3.2.1 swirl angle measurement

One of the primary objectives of this research was to measure the swirl flow angle along the test tube for different Reynolds number. The Reynolds number for these measurements ranged from 60,000 to 100,000 with L/D = 0 to 4. During the flow visualization test, it was observed that some of the water based liquid used to generate the smoke had condensed. This was deposited on the inside of the test tube wall in the form of droplets which followed the path of the swirl flow. Similar results were obtained by Sparrow(5) who injected an oil lamp black mixture onto a white plastic, self-adhering contact paper laid on the inside of the tube. By removing the paper, the angle made by the flow relative to the tube axis could be measured. In the present experiment, these were evaluated by placing a clear plastic sheet over the outside of the tube, tracing the streak lines and then measuring the angle in a similar to that of Sparrow(5). The movement of the droplets was, of course, due to the shear stresses exerted by the flow at the tube wall. The flow angles were measured at eight pre-selected locations along the length of the test section tube. The result for Re = 60,000 is shown in figure 6. In the figure, flow angles are plotted as a function of X/D for both of the extreme plenum chamber lengths(L/D = 0 and 4). Figure 6 illustrated the decay of the swirl angle along the tube, and hence the reduction of ratio of the tangential and axial shear stresses. The swirl flow starts with an angle of 70° with respect to the axial direction and decay to 55° at a location close to the end of the test section tube.

This angle would have been zero in the case of a pure axial flow. Inspection of the figures show that

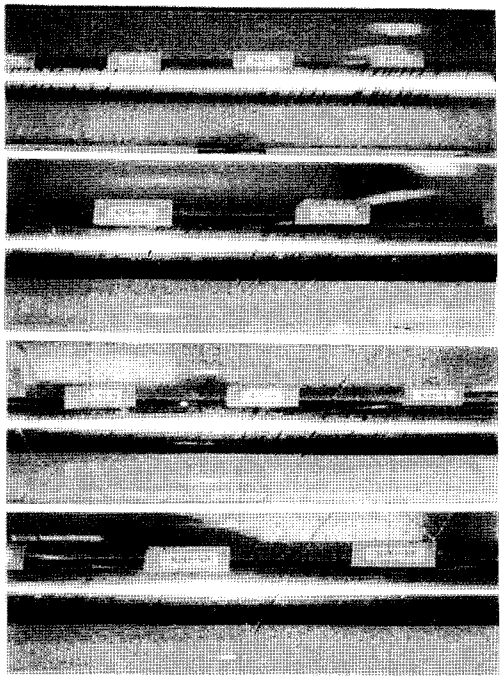

Fig. 6. Swirl Angle Distributions along the Test Tube by using Smoke for Re = 60,000 at L/D = 0 and X/D = 1~12

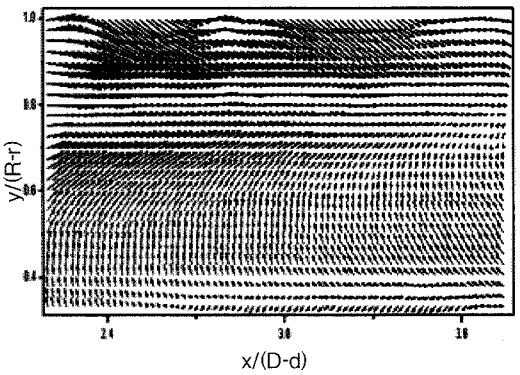

Fig. 7. Mean velocity vectors along the test Tube with swirl at x/(D-d)=30 for Re=20,000

θ decreases with X/D as before, and that increases in Reynolds number are accompanied by increases in the swirl angle θ. Of course, at any fixed values of X/D and Reynolds number, the swirl angle increases as L/D is increased and as the swirl intensity increase (i.e. L/D = 0 to 4). The fitted θ versus X/D equations were of the form

$$\theta = 64.285 + (7.216 \times 10^{-5}) \times \mathrm{Re} - 0.633\frac{L}{D} - 0.504\frac{X}{D}$$

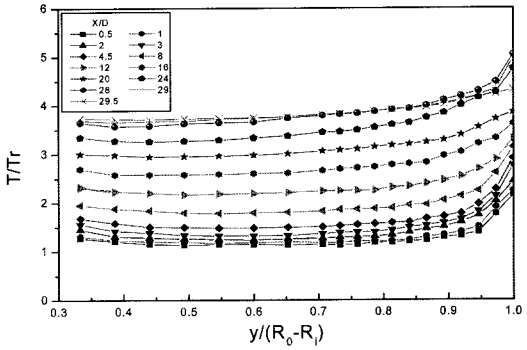

Fig. 8. Distributions of Temperature Profiles with swirl across the test tube for Re=30,000

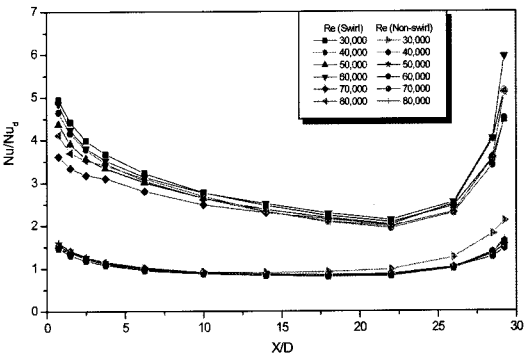

Fig. 9. Comparison o f Nusselt number with Swirl and without swirl for Re=30,000, 40,000, 50,000, 60,000, 70,000 and 80,000

3.2.2 Temperature and Nusselt number profiles in an annuli

Fig. 8 includes the local air temperature(T/Tr) of without swirling flow for Re=30,000.

For without swirling flow, the air temperature at consistent when X/D=0.5~4.5, y/(R0-Ri) = 0.7, but as X/D increased, T/Tr gradually increased. Near the concave tube wall, the air temperature sharply increased and appeared to increase further as the Reynolds number decreased.

Fig. 9 includes the comparisons between Nusselt number over the Reynolds number range Re=30000~80000 with swirling and without swirling flow. Nusselt number of swirling flow was observed to be 2.0~2.5 times bigger than the one for the without swirl flow at X/D=10~25. It also was observed to be 2.3~3.3 times bigger at the tube entrance and 3~4 times bigger at the end of the tube. It is thought that the swirling flow could

transfer more heat by fluid mixing due to tangential velocity. It means that the Reynolds number is a function of swirl intensity. If the Reynolds number is increased, the tangential velocity is increased and the heat transfer from the heated wall is also increased.

3.3 Velocity profiles at 90 degree circular bend

In a bend tube having peculiar geometry with curvature in the flow direction, strong flow occurs three dimensionally from the entrance of the tube and continues to exist until the exit of the tube. Fig 10 shows the time mean velocity vectors with swirl flow for 10,000 around the 90 degree tube. In Fig. 10, the straight line at entrance of the test tube represents the velocity vector at q = 0 degree, -6D~-7D. This shows that a negative velocity vector exists at y/D=0.4~0.7 in the test tube.

Along the test tube, the velocity vectors area moves toward the outer wall up to q=45 degree and then moves back to the inner wall. Passing through the bent tube, the negative velocity area of the velocity vector component changes in the center of the tube, and the swirl decays near the outlet of the tube.

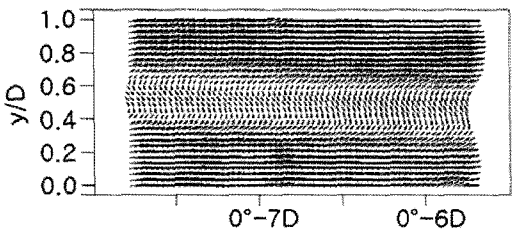

Fig. 10. Velocity vector distributions with swirl for Re=10,000 at q = 0~ -6D

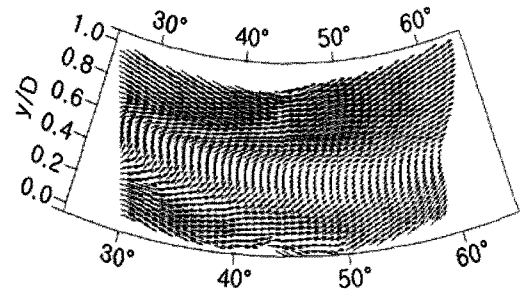

Fig. 11. Velocity vector distributions with swirl for Re=10,000 at bend angle=30~60

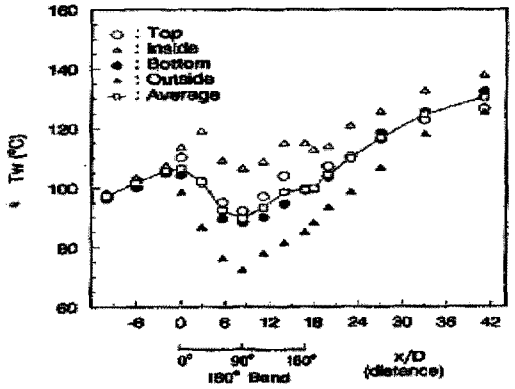

Fig. 12. Wall temperature profiles along the test tube without swirl for Re= 1×10^5

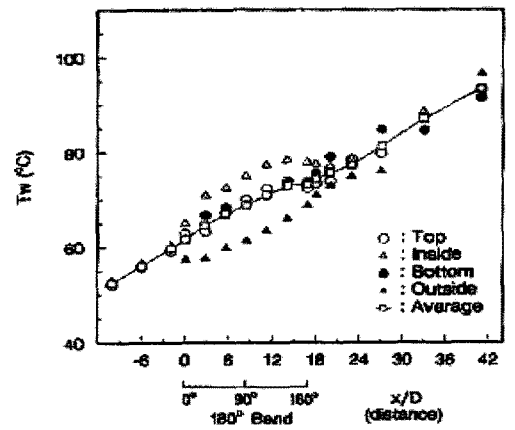

Fig. 13. Wall temperature profiles along the test tube with swirl for Re= 1×10^5

3.4 Heat transfer measurement at 180 degree circular bend

Fig. 12 shows the wall temperature profiles along the test tube without the swirl for Re=1×10^5.

There were temperature differences, between the inside and outside positions, similar to the without swirl flow, that started from the bend entrance but continually increased without decreasing unlike the without swirl flow.

If only considering the swirl flow, temperature profile is almost similar to that of the straight tube. Thus, the swirl flow is hardly affected by the geometrical shape of the bend and has heat transfer characteristics that are similar to those of the straight tube flow.

The Nusselt number was calculated from the wall and the bulk temperature of the upstream,

bend, and downstream of the test tube and made dimensionless by using the Dittus-Boelter equation for the fully developed flow, and the results are shown in Figs. 14 and. Fig. 15.

It is similar to the profile, which is suggested by Kays et al. (1980) to be reduced in *Nu/Nudb* at the straight tube of the upstream of the bend and at the inner and outer cross-sections of the tube bend entrance. It was shown that the maximum heat transfer occurred at 90° from the non-swirl flow, the *Nu/Nudb* increased, maximum at 90° and then decreased. In the swirl flow, the same trend occurred, but the *Nu/Nudb* was slightly bigger and less scattered than in the without swirl flow. It was shown that the swirl flow improves the heat transfer in the 180°bend flow.

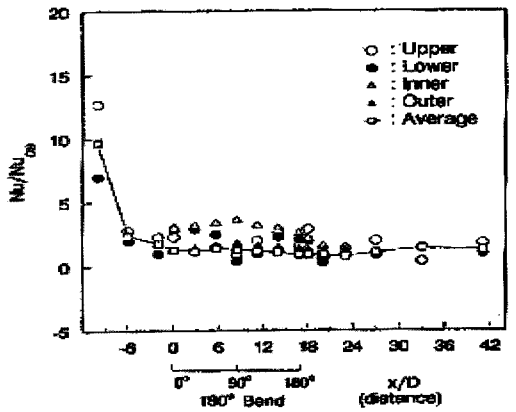

Fig. 14. Nusselt number profiles along the test tube with without swirl for Re=1×10^5

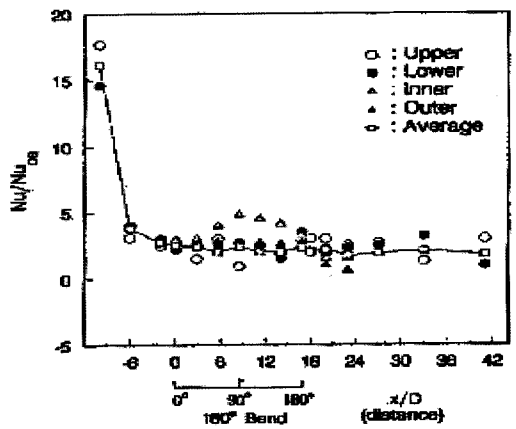

Fig. 15. Nusselt number profiles along the test tube with without swirl for Re=1×10^5

The Nusselt number for each Reynolds number of the inner and the outer positions of the bend tube in the without swirl flow are shown in Fig. 14. It was shown that the Nusselt number of the inner portion of the bend is 2.0 to 2.1 times greater than that at the outer position and maximum at 90° and then decreased.

3.5 Wake behind a round cylinder with swirl flow

An experimental study was performed on turbulent swirling flow behind a circular cylinder using 2-D PIV technique.

A comparisons was included with and without swirl flow behind a circular cylinder for Re= 10,000. The recirculation zones are shown unsymmetric profiles.

3.6 Temperature profiles using thermochromic liquid crystal

To determine some characteristics the turbulent flow. 2D PIV technique is employed for velocity

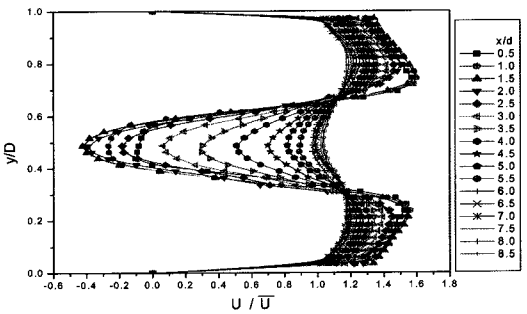

Fig. 16. Local Axial velocity profiles without swirl for Re = 10,000 behind the round cylinder

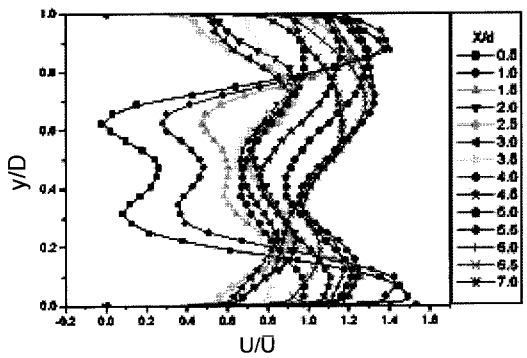

Fig. 17. Local axial velocity profiles with swirl for Re=10,000 behind the round cylinder

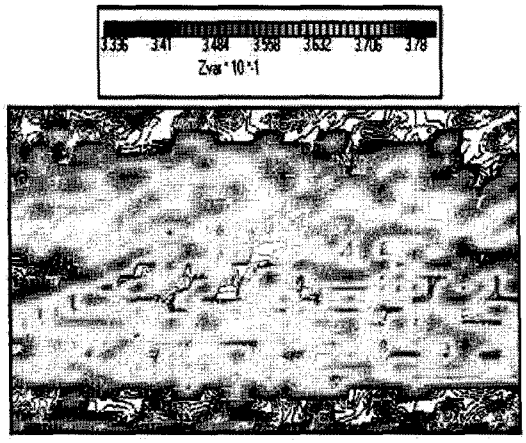

Fig. 18. Mean temperature distribution along the test tube using R. G. B at 36.5°C without swirl

Fig. 19. Mean temperature distribution along the test tube using R. G. B. at 36.0°C with swirl

measurement and liquid crystal is used for heat transfer experiments in water. Temperature visualization was made quantitatively calibrating the colour of liquid crystal versus temperature using various approaches. This study show the temperature and time-mean velocity distribution for Re=2436, 2500 and 2724 along longitudinal section and the results appear to physically reasonable.

4. Conclusion

Using 2D PIV technique, this study obtained the time mean velocity profiles and turbulent intensity with and without swirl flow for several Reynolds numbers. The author reached the following conclusions.

1. In general, the shape of the present axial velocity profiles are similar to those obtained by King's, Weske's and Khodadadai's in a straight circular tube.

2. The velocity vector had negative values near the convex tube and then the vectors changed to positive velocity after X/(D-d)=15.0 with decaying swirl intensity in an annuli. In the case of swirling flow, a strong 2-cell phenomenon appeared at the entrance of the test tube. The swirl decayed as it moved along the test tube, and then the peak streamwise mean velocity zone moved toward the convex tube wall.

3. The Nusselt number of swirling flow was observed to 2.0~2.5 times higher than one in fully developed region of the non swirl flow.

4. In the case 180 degree bend tube, The Nusselt number was the maximum a bend angle=90 degree and the Nusselt number at the inner portion of the cross-section of the tube was 2.0 to 2.3 times greater than that of outer position.

5. A comparisons was included with and without swirl flow behind a circular cylinder for Re=10,000. The recirculation zones are shown unsymmetric profiles.

6. Temperature visualization was made quantitatively calibrating the color of liquid crystal versus temperature using various approaches. This study show the temperature and time-mean velocity distribution for several Reynolds number along longitudinal section and the results appear to physically reasonable.

Acknowledgments

This study was supported financially by Ministry of Education, Science and Technology along with the Korean Institute of Science and Technology Information as a result of the Reseat program.

References

1) Lilley, D. G., 1973. Prediction of inert turbulent swirl flow. *AIAA*, Vol 11. No 7. pp 955-960.
2) Nuttal, J. B., 1953. Axial flow in a vortex. *Natural*, Vol 172. pp 582-583.
3) Binni, A. M., 1955. Experimental measement of flow swirling water through a pressure nuzzle and open trumpet. *Proc. of the Royal society*, Vol 235A. pp 78-88.

4) Chigier, N. A., and Chervinsky, A., 1967. Experimental investigation of swirling vortex motion in jet. *J. of Appl. Mechanics ASME*, Vol 34. pp 443-451.

5) Sparrow, E. M., and Chaboki, A., 1984. Swirl-affected fluid and heat transfer in a circular tube. *J. of heat transfer ASME* Vol 106. pp 766-773.

6) Chang, T. H., and Kim, H. Y., 2000. An investigation of swirling flow in a cylindrical tube. KSME International J. of mechanical science and technology Vol 15, pp 1892-1899.

7) Chighier A. N. and Beer J. M., 1964, Velocity and Static - Pressure Distributions in Swirling Air Jeys Issuing From Annular and Divergent Nozzle, *ASME, J. of Basic Engineering*, pp. 788- 796.

8) Scott C. J. and Raske D. R., 1973, Turbulent Viscosities for Swirling Flow in a Stationary Annulus , *ASME J. of Fluid Engineering*, pp 557 - 566.

9) Milar D. A., 1979, A Calculation of Laminar and Turbulent Swirling Flows in a Cylindrical Annuli, *ASME*, Winter Annual Meeting New York Dec. PP.89-98.

10) Clayton B. R., and Morsi Y. S. M., 1985, Determination of Principal Characteristics of Turbulent Swirling Flow Along Annuli , Int. J. Heat & Fluid Flow Vol.6, No.1, pp. 31-41.

11) Reddy, P. M., Kind R. J. and Sjolander S. A., 1987, Computational of turbulent swirling flow in an annular duct. Num. method in laminar and turbulent flow. pp 470-481.